Spectrum of first-nearest-neighbor Cr^{3+} pairs in ruby

J. P. van der Ziel
Bell Laboratories, Murray Hill, New Jersey 07974
(Received 30 August 1973)

The optical absorption, emission, and excitation spectrum and the exchange splittings of the first-neighbor Cr^{3+} pairs in Al_2O_3 have been studied. The earlier experimental level assignment is shown to be inconsistent with the theory of Pryce and Naito. The new ground-state level scheme is based on the σ-polarized fluorescence line at 7301.5 Å which terminates on the $S=2$ level, which is ~ 280 cm^{-1} above the $S=0$ level, and the π-polarized transition to the $S=3$ level at 7367.5 Å. The new parameters of the ground-state exchange $J(\vec{S}_1 \cdot \vec{S}_2)+j(\vec{S}_1 \cdot \vec{S}_2)^2$ are $J=54$ and $j=-8.7$ cm^{-1}. The infrared pair transitions obtain their strength mainly from the single-ion mechanism. The weakness of the exchange-induced dipole moment, which usually dominates in pair spectra, is attributed to a near cancellation of the single-electron components. A comparison of the relative σ and π intensities suggests that the odd-parity crystal field is somewhat different than for single ions. Transitions where both ions of the pair are excited to the ^2E states have been observed at nearly twice the R-line energy. The σ polarization of these transitions agrees with the exchange-induced dipole-moment mechanism. The temperature dependence of the absorption of the $S=0$ and 1 levels is in good agreement with the level populations derived from the ground-state exchange splittings.

I. INTRODUCTION

In heavily Cr^{3+}-doped Al_2O_3, a complicated pair luminescence and absorption spectrum is observed in addition to the sharp single-ion transitions between the single-ion $^4A_2$ and the two ^2E states.[1] There are four different types of near neighbors with a single intermediate oxygen ion, and these pairs have a sizable exchange interaction. The complexity of the spectrum has made it difficult to identify a given spectral line with a definite pair. After a considerable effort this identification is now nearly complete, and the level diagrams for the second- through fourth-neighbor pairs appear to be well established.[2] Rather little is known about the first-nearest-neighbor pair, even though, because of the relatively high D_3 symmetry, the excited-state exchange of this pair can be expressed in quite a simple form. Such a calculation has been made by Pryce[3] and by Naito[4] and the results are discussed in Sec. III. It is shown in Sec. IV that the theoretical predictions of the pair line polarization are inconsistent with the previous assignment of the first-neighbor spectrum. Using new experimental data, we propose a new ground-state level scheme which appears to be in better agreement with theory.

An additional complex absorption spectrum has been observed near 3400 Å by Linz and Newnham.[5] From the quadratic dependence on concentration of the absorption coefficient they deduced that this spectrum also involved Cr^{3+} pairs rather than single ions. On the basis of crystal-field calculations of Sugano and Tanabe,[6] they suggested that these transitions involved excited doublet states exchange coupled to the ground-state pair states. More recently it was shown that a line at 29 414 cm^{-1} corresponds to the single $^4A_2 \rightarrow {}^2A_1$ transition.[7-9] We have observed several strong σ-polarized transitions in the uv spectrum which are consistent with the simultaneous excitation of both ions of the first-neighbor pair to the ^2E states. The temperature dependence of the absorption is in reasonable agreement with the new ground-state splitting assignment.

II. PAIR SYMMETRY

Corundum belongs to the $D_{3d}^6 - R\bar{3}c$ space group, with the rhombohedral cell containing two Al_2O_3 units.[10] The Al^{3+} sites on which the Cr^{3+} ions substitute have approximately an octahedral coordination of oxygen ions. The site symmetry is C_3 and differs from C_{3v} only by a small rotation of the oxygen-ion triangles about the C_3 axis.

The geometry of the first-neighbor pair is shown in Fig. 1.[4] The pair has D_3 symmetry and in the (X, Y, Z) pair coordinate frame the Z axis has C_3 symmetry and passes through the two Cr^{3+} ions, and the X axis has C_2' symmetry and lies in the plane of the oxygen triangle and passes through one of the oxygen ions. There is an additional mirror plane midway between the ions if the distortions of the oxygen triangles are neglected. If the mirror plane is included the first-neighbor pair has the full D_{3h} symmetry of the Cr_2O_3 molecule. Figure 1 also shows several additional coordinate frames introduced by Naito.[4] The (x_b, y_b, z_b) axes are directed from the Cr^{3+} ions to the larger triangle of the O^{2-} ions, and in the octahedral approximation form the cubic bases in which the t_{2g} wave functions of the Cr^{3+} ions are defined. The basic (X_b, Y_b, Z_b) axes are obtained from

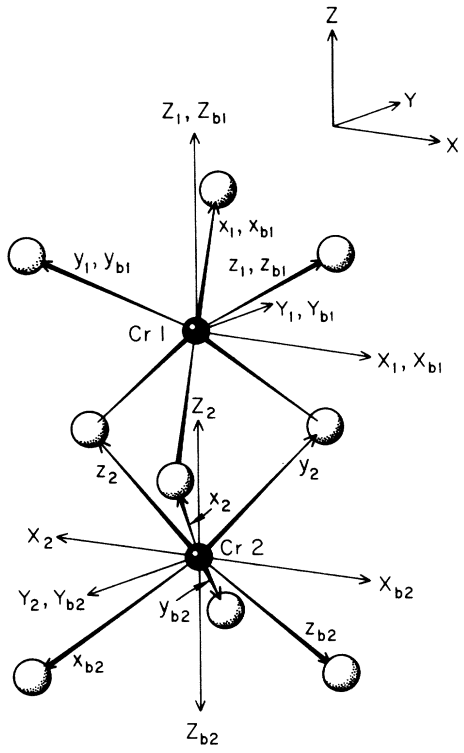

FIG. 1. First-nearest-neighbor Cr^{3+} pair in Al_2O_3. The coordinates discussed by Naito (Ref. 4) are shown.

(x_b, y_b, z_b) by a coordinate-axis transformation, and the (X, Y, Z) pair coordinate axes coincide with one of the ions of the pair. Coordinates (X_1, Y_1, Z_1) and (X_2, Y_2, Z_2), in which the Z axes of the pair are parallel, are used for the description of the angular momentum.

III. THEORY

A. Exchange interaction and crystal-field effects

The theory of the exchange interaction between Cr^{3+} pairs in ruby has been discussed by Pryce[3] and by Naito.[4] In this section we will quote the results of the calculations which are pertinent to the first-neighbor pair system. Naito has shown that the usual bilinear exchange interaction between two ions with singly occupied orbitals must be modified in the multielectron case to include the effects of how the remaining spins are coupled. These effects are incorporated by including biquadratic terms and the exchange is

$$\mathcal{H}_{ex} = \sum_{j,k} J_{1j,2k}\vec{s}_{1j}\cdot\vec{s}_{2k} + \sum_{i\neq k,\, j\neq l} J_{1i2j,1k2l}(\vec{s}_{1i}\cdot\vec{s}_{2j})(\vec{s}_{1k}\cdot\vec{s}_{2l})$$
$$+ \sum_{i\neq j\neq k} \{J_{1i1j,1k2l}(\vec{s}_{1i}\cdot\vec{s}_{1j})(\vec{s}_{1k}\cdot\vec{s}_{2l})$$
$$+ J_{2i2j,2k1l}(\vec{s}_{2i}\cdot\vec{s}_{2j})(\vec{s}_{2k}\cdot\vec{s}_{1l})\}$$
$$+ \sum_{i\neq j,\, k\neq l} J_{1i1j,2k2l}(\vec{s}_{1i}\cdot\vec{s}_{1j})(\vec{s}_{2k}\cdot\vec{s}_{2l}) . \quad (1)$$

Here $\vec{s}_{1i}$ is the single-electronic-spin operator acting on the ith orbital of the first Cr^{3+} ion. The sums are over the three t_{2g} orbitals which make up the $^4A_2$ and ^2E states and whose strong crystal-field states transform as $\xi \sim d_{yz}$, $\eta \sim d_{zx}$, and $\zeta \sim d_{xy}$ for $i = 1, 2, 3$, respectively. The biquadratic exchange parameters J_{ijkl} are significantly smaller than the J_{ij} and the effect of these terms is to introduce small shifts in the energies determined from the first term.

Equation (1) is invariant under the symmetry operation of D_3 and it follows that the orbital exchange parameters fall into three groups:

$$J_{11} = J_{22} = J_{33} ,$$
$$J_{12} = J_{23} = J_{31} , \quad (2)$$
$$J_{21} = J_{32} = J_{13} .$$

The additional relation $J_{12} = J_{21}$ is obtained for the D_{3h} symmetry. Thus, neglecting the small differences between J_{12} and J_{21}, the major contributions to the exchange splittings are determined by two groups of parameters.

Let the t_{2g} orbitals be defined in the idealized octahedral coordinate frame shown in Fig. 1. For this geometry the integral giving J_{11} results from the direct overlap of the d^1_{yz} and d^2_{yz} orbitals. The first of the semiempirical Goodenough and Kanamori rules leads us to expect that this exchange will be strongly antiferromagnetic.[11] There is no direct overlap between the orbitals d^1_{yz} and d^2_{xz} and, furthermore, the overlap with the oxygen p orbitals is also small so that the total probability of electron transfer is small. Thus, from the second Goodenough and Kanamori rule, we expect J_{12} to be ferromagnetic with $|J_{12}| < J_{11}$.

The total spin $\vec{S} = \sum_j (\vec{s}_{1j} + \vec{s}_{2j})$ and the Z component of the spin, m, along the C_3 axis commute with Eq. (1) and the pair wave functions are defined in terms of these quantum numbers. We let M be the "+, −" orbital components of the ^2E state. The wave function is

$$|gSm\rangle = |{}^4A_2\,{}^4A_2 Sm\rangle \quad (3)$$

for the ground state,

$$|e_M Sm\rangle = |{}^2Eu_M\,{}^4A_2 Sm\rangle , \quad (4a)$$
$$|\bar{e}_M Sm\rangle = |{}^4A_2\,{}^2Eu_M Sm\rangle \quad (4b)$$

for the singly excited pair, and

$$|e_M e_{M'} Sm\rangle = |{}^2Eu_M\,{}^2Eu_{M'} Sm\rangle \quad (5)$$

for the doubly excited pair states.

The single-ion $^4A_2$ and ^2E states are split by the combined effect of the trigonal crystal field and the spin-orbit interaction. For nearest neigh-

bors the anisotropy energy of the ^2E state is given by

$$\mathcal{H}_{AE} = \lambda[T_1 S_{1z} + T_2 S_{2z}], \tag{6}$$

where for ion 1 of the pair T_1 is an operator which is diagonal in the u_M components of E with eigenvalues ± 1, and S_{1z} operates on the z component of the spin.[6] For the singly excited pair states Eq. (6) has diagonal matrix elements $\pm m\lambda/4$ for each S value, and off-diagonal elements $\pm \lambda(4-m^2)^{1/2} \times \delta(M, M')/4$ between states of different S. For the states of the doubly excited pair there are diagonal matrix elements $m\lambda\delta(M, M')$ for $S=1$ and off-diagonal elements $\pm\lambda$ between states with $S=1$ and $S=0$ for $m=0$ and $M \neq M'$.

Experimentally the splittings due to crystal anisotropy are found to be quite small for the first-neighbor pair. This can be understood as follows: McClure has found that the trigonal field parameter is a very sensitive function of position of the Cr^{3+} ion in the lattice.[12,13] For the single ion, $\lambda = 29\ cm^{-1}$ and a value of the trigonal field parameter v of $\sim 1425\ cm^{-1}$ is obtained from the splitting of the ^4T bands. This is consistent with a slight displacement of the ion from the Al^{3+} equilibrium position. In Cr_2O_3 the splitting of the ^4T bands yields $v \sim -700\ cm^{-1}$, which not only is smaller but also has the opposite sign. The trigonal field of the first-neighbor ions is expected to have an intermediate value; thus the ^2E splittings will be considerably smaller than the single-ion splitting. The relative smallness of the crystal anisotropy enables us to neglect this effect in calculating the energies.

Within the $^4A_2$ state, Eq. (1) can be written

$$\mathcal{H}_{ex} = J'(\vec{S}_1 \cdot \vec{S}_2) + j(\vec{S}_1 \cdot \vec{S}_2)^2 + j''' - 63j/16, \tag{7}$$

where the j's are defined in Ref. 4 and $J' = J + \frac{1}{2}j + j' + j''$.

Making use of Eq. (2), the dominant bilinear exchange expressed in terms of the single-electron exchange parameters is

$$J = (J_{11} + J_{12})/3\ . \tag{8}$$

The term biquadratic in the spins in Eq. (7) is due to the correlational dependence of the exchange. Several calculations have shown that j may be of the order of 1% of J and is probably smaller than this in most cases.[14] There is, however, a formally similar term which results from exchange striction. This effect yields a negative contribution to j, and in all cases appears to dominate over the correlational contribution.[14–17]

The pair wave functions of the ground state are given by $|Sm\pm\rangle$, where the "±" refers to the parity under the interchange of the two ions. States with $S=3$ and 1 have "+" parity, while those with $S=2$ and 0 have "−" parity.

For the single excited states the matrix elements of the Hamiltonian, Eq. (1), which neglect excited-state striction effects can be expressed in the form

$$\mathcal{H} = R' + \begin{array}{c} \begin{matrix} |e_+\rangle & |e_-\rangle & |\bar{e}_+\rangle & |\bar{e}_-\rangle \end{matrix} \\ \begin{bmatrix} 0 & 0 & \frac{9}{4}K_1 & 0 \\ 0 & 0 & 0 & \frac{9}{4}K_1^* \\ \frac{9}{4}K_1^* & 0 & 0 & 0 \\ 0 & \frac{9}{4}K_1 & 0 & 0 \end{bmatrix} \end{array} + \begin{bmatrix} J'' & 0 & K_2 & 0 \\ 0 & J'' & 0 & K_2^* \\ K_2^* & 0 & J'' & 0 \\ 0 & K_2 & 0 & J'' \end{bmatrix} [\tfrac{1}{2}S(S+1) - \tfrac{9}{4}], \tag{9}$$

where

$$\begin{aligned} R' &= R - 2j''' + \tfrac{51}{16}j\ , \\ J'' &= J - 4j'\ , \\ K_1 &= K + 2k' - \tfrac{1}{6}k_1 - \tfrac{1}{9}k_2\ , \\ K_2 &= K + 2k' + \tfrac{1}{2}k_1 + \tfrac{5}{3}k_2\ . \end{aligned} \tag{10}$$

The j's and k's are sums over the biquadratic exchange terms which result from the correlational effect.[4] These terms are probably quite small compared with the exchange striction effect, which will contribute to both the diagonal and off-diagonal terms, and these latter contributions may be of the same order as for the ground state and may thus be quite important. However, since the amount of information about the excited-state levels is limited, the striction effect in the excited state will not be considered further here. In this order of approximation $K_1 = K_2 = K$, which in terms of the single-electron exchange parameters is

$$K = (J_{11} - J_{12})/6\ . \tag{11}$$

The excited-state exchange parameters may well be somewhat larger than for the ground state because of a slight dilatation of the t_{2g} wave functions in the ^2E state, which will increase the overlap integral significantly, and the slightly smaller energy denominator in the theoretical expression for the exchange. Thus, the exchange parameters should be considered as empirical quantities for each state.

The signs of the exchange parameters obtained from the Goodenough–Kanamori rules[11] indicate $K>0$ and Fig. 2 shows the normalized exchange splittings plotted as a function of K/J. Experimentally we will show that the $|2-\rangle$ singly excited

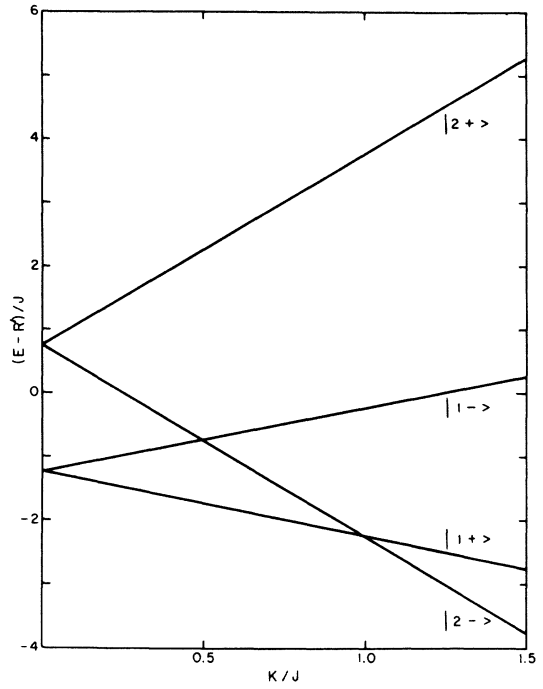

FIG. 2. Exchange splitting of the singly excited states as a function of K/J.

level lies below the $|1+\rangle$ level, implying $J_{11} < -5J_{12}$.

Each of the four levels consist of two degenerate states obtained from $|e_+\rangle$ and $|e_-\rangle$ and each has an additional $(2S+1)$-spin degeneracy. The wave functions of the single excited pair are classified according to e_M, S, m, and the "±" parity under interchange of particles,

$$|SmM\pm\rangle = (|e_M Sm\rangle \pm |\bar{e}_M Sm\rangle)/\sqrt{2} \ . \qquad (12)$$

The crystalline anisotropy effects are relatively small and hence the energies are independent of m and M. Consequently the levels in Fig. 2 are simply identified by $|S\pm\rangle$.

For the doubly excited pair levels, we neglect all biquadratic exchange and striction effects and retain only the bilinear exchange. The energies in this approximation are obtained from diagonalization of

$$\mathcal{H} = 2R' + \begin{array}{c} \begin{matrix} |e_+e_+\rangle & |e_+e_-\rangle & |e_-e_+\rangle & |e_-e_-\rangle \end{matrix} \\ \begin{bmatrix} J & 0 & 0 & 0 \\ 0 & J & 8K & 0 \\ 0 & 8K^* & J & 0 \\ 0 & 0 & 0 & J \end{bmatrix} \end{array} \times [\tfrac{1}{2}S(S+1) - \tfrac{3}{4}], \qquad (13)$$

where the $|e_M e_{M'}\rangle$ are defined in Eq. (5). The normalized exchange splitting as a function of K/J is shown in Fig. 3. The resonant interaction K couples the states $|e_+e_-\rangle$ and $|e_-e_+\rangle$ and the wave functions of these states are

$$|S\pm\rangle = (|e_+e_- Sm\rangle \pm |e_-e_+ Sm\rangle)/\sqrt{2} \ . \qquad (14)$$

The states with $M = M'$ are not coupled by off-diagonal elements. According to Eq. (13) the states have a twofold orbital degeneracy. Under an interchange of particles, these $S=1$ and 0 states have even and odd parity, respectively, and are denoted in Fig. 3 by $|1(+)\rangle$ and $|0(-)\rangle$.

B. Transition dipole moment

We have shown that the wave functions are classified as either symmetrical (+) or antisymmetrical (−) with respect to the interchange of the two ions. From the D_3 symmetry we obtain that, no matter what the electric dipole moment mechanism, π-polarized transitions are only allowed between states of opposite parity, and σ-polarized transitions between states of the same parity.

Transitions between the pure single-ion $^4A_2$ and ^2E states are spin and parity forbidden but become allowed by the admixture of the odd-parity crystal field and the spin-orbit interaction.[6] The single-ion selection rules are $\Delta S = 0, \pm 1$, $\Delta m = 0, \pm 1$. Since the second ion of the pair is not affected as the first undergoes a transition by this mechanism, these selection rules also apply to the singly excited pair states. The squares of the matrix ele-

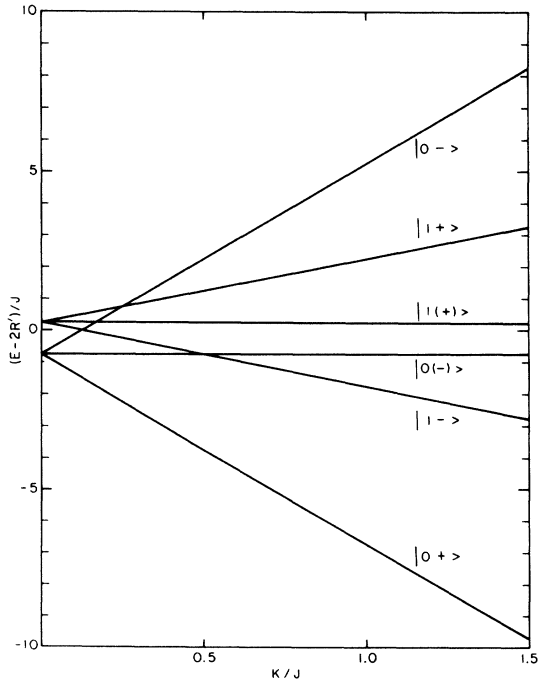

FIG. 3. Exchange splitting of the doubly excited states as a function of K/J.

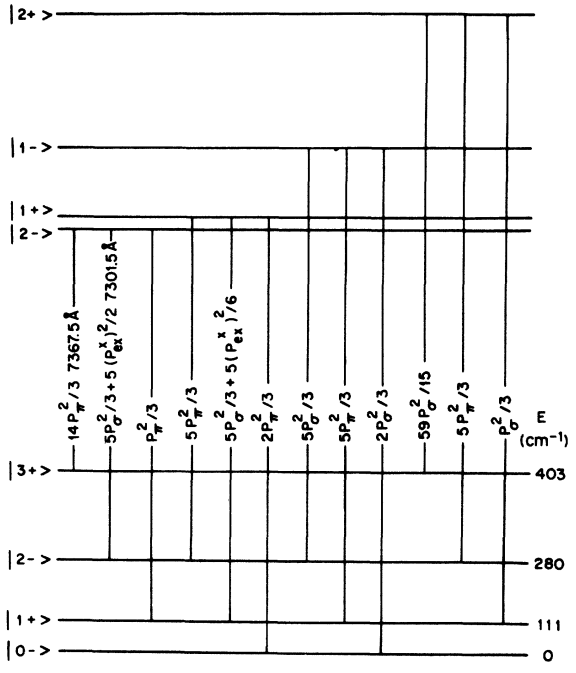

FIG. 4. Squares of the matrix elements of the dipole moments to the singly excited state. The squares of the matrix elements for the individual components are listed in the Appendix. The two pair transitions and the ground-state splittings obtained from $J=54$ and $j=-8.7$ cm^{-1} and also shown.

ments of the single-ion transition dipole moment are given in the Appendix, and are shown in Fig. 4.

The exchange-induced dipole moment[18]

$$\vec{P}_{ex}=\sum_{ij}\vec{\pi}_{ij}(\vec{s}_i\cdot\vec{s}_j) \tag{15}$$

contributes to the transition strength of some of the single excited states, and is the sole mechanism responsible for the transition moment to the doubly excited states.[19,20] The selection rules of Eq. (15) are $\Delta S=0$ and $\Delta m=0$. Using the trigonal symmetry of the pair we obtain symmetry relations between the $\vec{\pi}_{ij}$ analogous to the J_{ij} in Eq. (2). For example, applying the C_2' operation along the X direction of the pair we find $\vec{\pi}_{33}$, $\vec{\pi}_{12}$, and $\vec{\pi}_{21}$ are parallel to the X axis, and thus appear only in σ polarization.[3]

The remaining $\vec{\pi}_{ij}$ are obtained from application of the C_3 and C_3^2 operations and these dipole moments lie along the two other C_2' axes. Thus, if the dipole moments were simply additive, they would vanish by cancellation. However, in the $|1+\rangle$ and $|2-\rangle$ singly excited states as well as the $|0(-)\rangle$ and $|1(+)\rangle$ doubly excited states the pair wave functions contain an appropriate phase relationship so that the matrix elements of Eq. (15) do not cancel for symmetry reasons. For the singly excited state we let

$$P_{ex}^{X}=\pi_{33}^{X}+\tfrac{1}{2}(\omega+\omega^2)(\pi_{12}^{X}+\pi_{21}^{X}), \tag{16}$$

where $\omega=e^{2\pi i/3}$ and the superscript denotes the X direction of the dipole moment. For the doubly excited states the phase relations are somewhat different and

$$P_{ex}^{X'}=\pi_{33}^{X}+\pi_{12}^{X}+\pi_{21}^{X}\,. \tag{17}$$

The squares of the exchange-induced dipole moments are given in the tables in the Appendix and the total dipole strength of the transitions to the singly excited states are shown in Fig. 4.

IV. EXPERIMENTAL DETERMINATION OF SINGLY EXCITED PAIR LEVELS

A. Comparison of earlier work with theory

Using the piezospectroscopic method, Mollenauer and Schawlow have unambiguously identified two of the first-neighbor lines in the low-temperature luminescence spectrum.[21] These are the intense broad lines at 7540 Å which appear in π polarization and a weak line at 7302 Å in σ polarization. The emission was identified with transitions originating on the lowest-energy singly excited state and terminating on the $S=2$ and 1 ground-state levels, respectively. They thus deduced that for the ground state $J\sim225$ cm^{-1}. Based on considerably weaker evidence they found three other lines in emission and absorption which could also be identified with the first neighbors. Their energy-level diagram is shown in Fig. 5 and the ground-state splittings of this assignment yield $J=185.7$ cm^{-1} and $j=-8.7$ cm^{-1}.

Let us compare this assignment with the theoretical results of Sec. III. The complete polarization

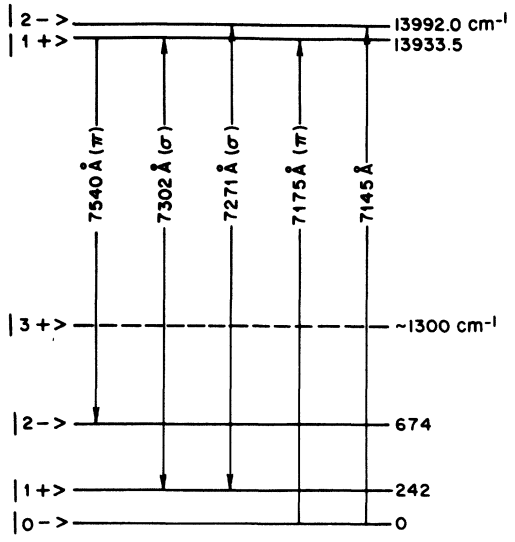

FIG. 5. First-nearest-neighbor energy diagram after Mollenauer and Schawlow (Ref. 21).

of the 7540- and 7302-Å lines agrees with theory, and the level assignment is explained if the luminescence originates on the $|1+\rangle$ state. However, according to a more recent investigation by Engstrom the 7271-Å emission is at least partly σ polarized, and this is inconsistent with polarization rules for the transition from the $|2-\rangle$ excited state to the $|1+\rangle$ ground state.[22,23] The 7175-Å line of Mollenauer and Schawlow has the correct π polarization for the $|1+\rangle$ to $|0-\rangle$ transition. However, Engstrom has identified a line at 7177.0 Å, which is presumably the same line, with the $S=1$ ground-state level from temperature-dependent absorption data. The 7145-Å line was not observed by Engstrom, and its polarization is not known. The line is identified with the transition from $|2-\rangle$ to $|0-\rangle$ which is forbidden by the theory of Sec. III, and the assignment of this transition is deemed to be questionable as well.

The discrepancies between theory and experiment lead us to question the identification of the less-well-established first-neighbor transitions, and suggest that the pair spectrum be reexamined for an alternative assignment. Figure 4 indicates that the strongest π-polarized dipole strength occurs for the transition between the $|2-\rangle$ excited state and the $|3+\rangle$ ground state. We could tentatively identify this transition with the 7540-Å line, and further identify the 7302-Å line with the $|2-\rangle$ to $|2-\rangle$ transition, and thus obtain $J \approx 143$ cm^{-1}.

One difficulty with the new identification is the temperature-dependent absorption data of the 7302-Å line obtained by Mollenauer and Schawlow which indicates this level is 240 ± 40 cm^{-1} above the $S=0$ level.[21] We have estimated the error from the scatter of their data. The line is very weak in absorption, and the accuracy of the absorption measurement was relatively low. Nevertheless, this value is quite different from the value ~428 cm^{-1} obtained for the alternative assignment. This alternative value for the ground-state exchange splitting is not very different from the second-neighbor splittings. Thus some lines previously attributed to the second-neighbor pairs may, in fact, originate on the first neighbors. However, as we show in Sec. IV B the identification of the 7540-Å line with an electronic transition also appears to be incorrect.

B. New experimental work

In previous studies of the first-nearest-neighbor Cr^{3+} pairs in $LaAlO_3$ and $YAlO_3$ it was found that, compared to the emission from single ions, as well as the more-distant-neighbor pairs, the nearest-neighbor emission intensity is greatly enhanced by selectively exciting the doubly excited pair states.[20,24] Furthermore, by monitoring the luminescence of different pair lines one can iden-

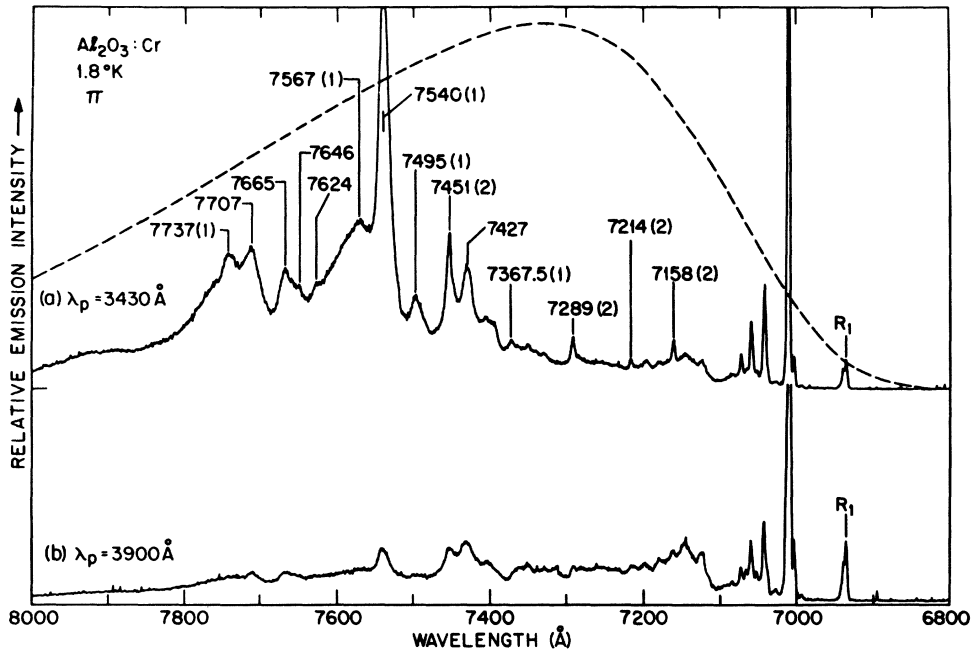

FIG. 6. π-polarized emission at 1.8°K for excitation into (a) the 3430-Å doubly excited levels of the first-neighbor pair, and (b) the $^4T_1$ band of the single ions. The spectral response of the luminescence detection system is shown by the dashed line. The first- and second-neighbor transitions as deduced from the relative intensities as well as stress experiments are denoted by (1) and (2), respectively.

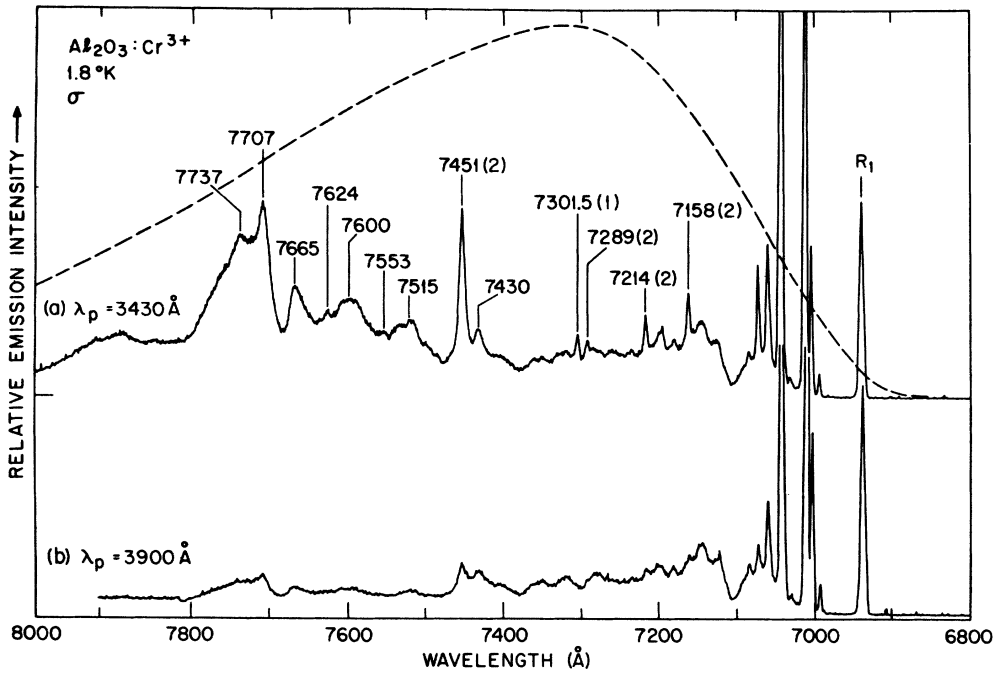

FIG. 7. σ-polarized emission at 1.8 °K for similar excitation as in Fig. 6.

tify the lines in the excitation spectrum with the type of neighbor. A similar experiment was recently reported in ruby by Kushida and Tanaka, who examined the excitation spectrum of the single ion, as well as the third- and fourth-neighbor emission, using a tunable dye laser in the B-line region between 4600 and 4900 Å as the excitation source.[25] In another experiment the emission intensities of

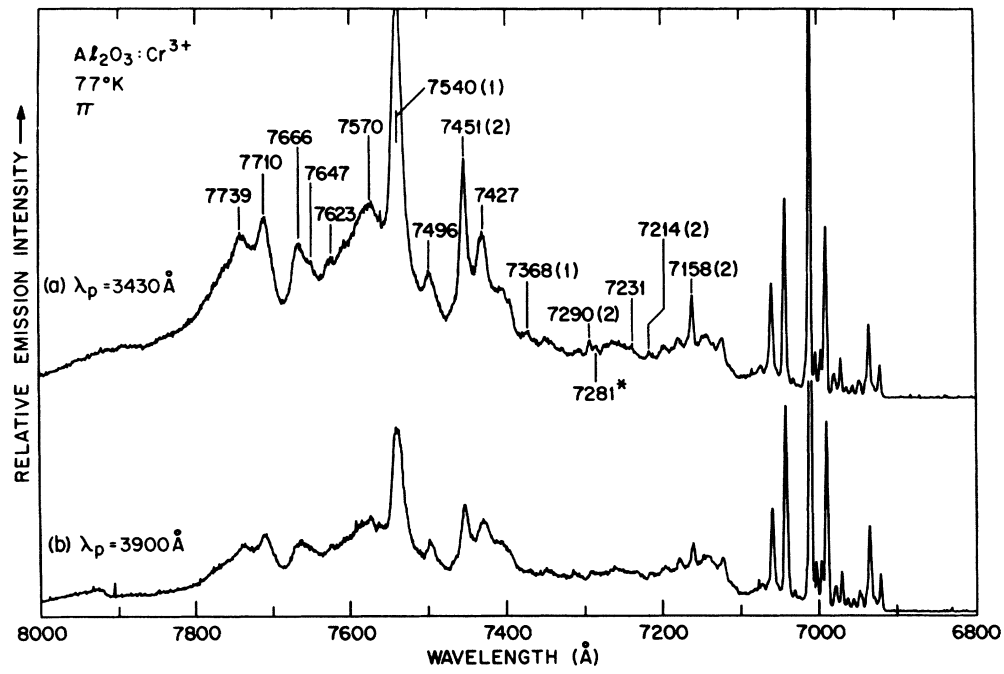

FIG. 8. π-polarized emission at 77 °K for similar excitation as in Fig. 6. Emission from the higher-energy singly excited levels is shown by an asterisk.

the first and second neighbors were found to be enhanced using a 3371-Å N_2 laser source.[25]

We have also observed an enhancement of the pair emission for excitation into the doubly excited pair states near 3430 Å. The excitation source was a $\frac{1}{4}$-m Bausch and Lomb spectrometer equipped with a 150-W xenon arc lamp. The luminescence was detected using a 1-m Czerny-Turner spectrometer and a cooled *S*-20 response photomultiplier tube. According to theory, the optimum enhancement of the first-neighbor lines is obtained when the pump radiation propagates along the *c* axis of the crystal and hence is completely σ polarized. The σ and π components of the luminescence were detected in an orthogonal direction.

The luminescence spectra from a ruby with 0.9-wt% Cr^{3+} which were obtained by exciting the doubly excited ion band at 3430 Å as well as the predominantly single-ion $^4T_1$ band, which peaks at ~3900 Å, are shown in Figs. 6–9, and the numerical data are shown in Table I. In order to facilitate the comparison, the slit width of the excitation source was adjusted to yield about the same *R*-line intensity. The spectral response of the detection system was also modified by glass filters, and the response curves, which were calibrated using a standard lamp, are given by the dashed lines in Figs. 6 and 7.

The ratios of the intensities of the emission under 3430- and 3900-Å excitation obtained from Figs. 6 and 7 are listed in Table I. From Fig. 6, we see that the enhancement of the 7540- and 7451-Å lines is 12 ± 1 and 5.2 ± 0.6, respectively, and this is to be compared with an *R*-line intensity ratio of 0.55 ± 0.05. Thus, the enhancement of the 7540-Å line is significantly higher than for the second neighbors, indicating that the 3430-Å band corresponds predominantly to first-nearest-neighbor absorption.

An enhancement similar to that of the 7540-Å line is also found for the π-polarized 7367.5-, 7495-, 7567-, and 7737-Å lines, suggesting that this emission is also associated with the first-neighbor system. The enhancement of the 7158-, 7214-, 7289-, 7515-, 7600-, 7624-, 7665-, and 7707-Å lines is similar to the enhancement of the 7451-Å line indicating that these lines may be associated with the second-neighbor system. The intensity of the pair lines relative to the *R* lines is a very sensitive function of the wavelength and slit settings of the excitation spectrometer. Thus, in Fig. 7, which was obtained using slightly different settings than Fig. 6, the *R*-line intensity ratio is 0.85 ± 0.08, while the ratios of the first-neighbor lines at 7301.5 Å and the 7451-Å line at 7451 Å are 12.4 and 5.7, which are only slightly larger than the ratios of Fig. 6.

In passing we note that the 7158- and 7289-Å lines are quite evident in the 1.8 °K spectrum. This observation is inconsistent with the second-neighbor assignment of Kisliuk *et al.*,[2] who identi-

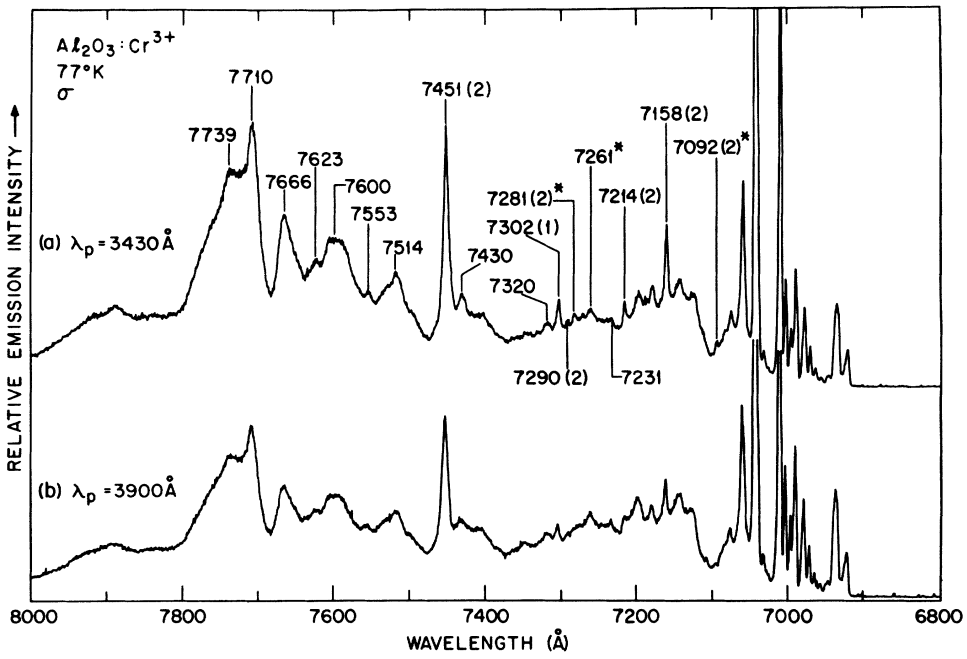

FIG. 9. σ-polarized emission at 77 °K for similar excitation as in Fig. 6. Emission from the higher-energy singly excited levels is shown by an asterisk.

TABLE I. Energy levels obtained from the 1.8 °K fluorescence spectrum (Figs. 6 and 7). The neighbor assignment is derived from the enhancement of the fluorescence intensity under excitation into the doubly excited pair states near 3430 Å relative to excitation at 3900 Å.

Wavelength (Å)	Predominant polarization	$\frac{\delta E}{\delta P}\left(\frac{\text{cm}^{-1}}{100\ \text{kg/mm}^2}\right)$	uv intensity enhancement (±10%) Fig. 6	Fig. 7	Neighbor assignment	Comments
6934			0.5	0.86		R_1
7122	U		0.49			
7145	U	−2.3		0.87		Vibr. of R_1
7158	U	+2.8	4	5.2	2	
7177	U			0.9		Present at 1.8 °K
7194	U	−5.9		3		
7214	U	+3.3		5	2	
7231	U					
7289	U	+6.4	4.6	5.1	2	Present at 1.8 °K
7301.5	σ	−27		12.4	1	$S=2-$ to $2-$
7320	σ					
7329	U	+5.4				
7367.5	π	−22.5	12.5		1	$S=2-$ to $3+$
7427	π		2.5			
7430	σ			~1.6		
7451	U	+12	5.2	5.7	2	
7495	π	−21.8	12		1	Vibr. of 7367.5
7515	σ	+5.4		~5	2	
7540	π	−22.4	12		1	Vibr. of 7367.5
7553	σ					
7567	π	−22.3	~12		1	Vibr. of 7367.5
7600	σ			~5	2	
7624	U		5	5	2	
7646	π					
7665	U	+5.7	5	5.5	2	
7707	U	+7.3	6		2	
7737	U	−22.1	11		1	Vibr. of 7367.5

fied these lines as originating on higher-energy excited-state pair levels rather than the lowest-energy excited level which is consistent with our observations. The crystal was immersed in the liquid helium, and was not sufficiently heated by the pump radiation to populate the levels which are approximately 106.5 and 107.5 cm^{-1} above the lowest-energy excited level from which this emission was presumed to originate.[2] This leads us to suspect their second-nearest-neighbor assignment, and the subsequent theoretical interpretation of Naito.[4]

The 7540-Å line has a width at half-intensity of ~14 Å, which is considerably broader than the widths of the other pair lines, and has an asymmetric line shape with an apparent low-energy cutoff. The more dilute rubies have narrower lines, and with a 0.093-wt% Cr^{3+} crystal, this emission is resolved into two lines at 7541.7 and 7536.8 Å (Fig. 10). The lines scale similarly with excitation energy and are thus both identified with the first-neighbor pair. The temperature independence of the emission indicates that the 8.6-cm^{-1} splitting does not originate in the excited state. This splitting also appears to be too large to be due to the crystal-field effect in the ground state. These results, together with the anomalously strong intensity relative to the 7301.5-Å line, suggest that the 7540-Å emission is a vibronic rather than an electronic no-phonon line. We identify the 7367.5-Å line as the no-phonon origin of this first-neighbor line.

Confirmation of this assignment is obtained from the shift of the lines under compression along the c axis. The 7540-Å emission shifts by -22.4 ± 0.8 cm^{-1} for an applied stress of 100 kg/mm^2 and this agrees with the shift of -22.8 cm^{-1} of Mollenauer and Schawlow.[21] The 7367.5-Å line as well as the other long-wavelength lines identified in Fig. 6 and by Table I (1) exhibit similar red shifts.[26] Together with the enhancement under uv excitation, the latter data thus indicate that these

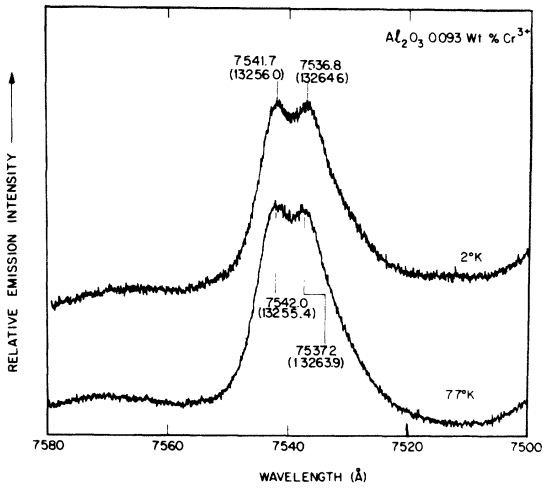

FIG. 10. Resolution of the first-neighbor emission at 7540 Å into two components.

lines are also vibronics of the 7367.5-Å transition.

Mollenauer and Schawlow observed that the shift with pressure of the 7301.5-Å line was about half of the shift of the 7540-Å line or ~ -11.4 cm^{-1} per 100 kg/mm^2. In contrast we observe this line to shift -27 ± 1.5 cm^{-1} under this pressure. In the same measurement the shift of the 7450-Å line is found to be $+12 \pm 1$ cm^{-1} per 100 kg/mm^2, which agrees with the value of 13.5 cm^{-1} obtained by Mollenauer and Schawlow.[21]

The relative intensities of the 7367.5- and 7301.5-Å lines are also of interest. Unlike the Cr^{3+} pair spectrum in $LaAlO_3$,[20] $YAlO_3$[24] and the third and fourth neighbors in ruby,[2] the exchange-induced dipole moment is not the dominant transition mechanism. Since a large dipole moment is observed for the doubly excited states, there appears to be a cancellation of the type $(\pi^X_{12} + \pi^X_{21})/2 \approx \pi^X_{33}$ which results in the small exchange-induced dipole moment of the singly excited state.

The single-ion transition to ^2E obtains its strength via the spin-orbit coupling to the $^4T_2$ state.[6] The σ component of $^4T_2$ derives from the C_{3v}- and C_3-symmetry odd-parity crystal field, and the π component results only from the C_3 odd-parity crystal field.[12] The odd-parity components are sensitive functions of the position of the ion and will thus be somewhat different for the single ion and the first-neighbor pair. However, we can obtain a rough estimate of the relative intensities if we use the relationship between the σ and π intensities of the single ion and neglect the contribution of the exchange-induced dipole moment. Using the experimental intensities of the $^4T_2$ transitions, the calculated strengths of the ^2E transitions correspond to a polarization ratio $(P_\sigma/P_\pi)^2 = \frac{8}{3}$.[27] However, a large fraction of the π component of $^4T_2$ is vibronically induced, and this does not contribute to the π component of the R lines. The experimental ratio of the total R-line intensity is found to be $(P_\sigma/P_\pi)^2 = \frac{8}{3} \times 3.2$.[27]

Using the experimental single-ion ratio and assuming the $|2-\rangle$ excited state is lowest, the transitions to $|2-\rangle$ and $|3+\rangle$ yield a σ/π intensity ratio from the single-ion mechanism of ~ 3. This ratio is ~ 8.5 for the transitions from the $|1+\rangle$ excited state to $|2-\rangle$ and $|1+\rangle$. The presence of a σ-polarized exchange-induced dipole-moment contribution will tend to increase this ratio. The experimental ratio at 77 °K, corrected for the response of the system, is 2.1 ± 0.7, and this can be reasonably ascribed to the $|2-\rangle$ excited state having the lowest energy. The smaller value of the ratio suggests that the C_3 component of the odd-parity crystal field is larger relative to the C_{3v} component for the first neighbors than it is for the single ions.

On the basis of our assignment the remaining π-polarized transition to the $|1+\rangle$ is expected to be ~ 7212 Å. This is close to the 7214-Å line which we have identified with the second-neighbor spectrum. The fact that this transition is not observed is not surprising since its intensity is predicted to be down by a factor 14 as compared to the transition to $|3+\rangle$. On the other hand, if the $|1+\rangle$ excited state had the lowest energy, the intensity ratio of the π-polarized lines would be $\frac{2}{5}$ and this transition should have been observed. This thus provides additional confirmation that the $|2-\rangle$ state has the lowest energy.

The absence of the third line at low temperatures could also result from the crystal-field splittings of the excited states. From Table V, it is seen that if the $|2-\rangle$ state is lowest and with a negative λ, strong emission will be observed to the $S=3$ level. The intensity of the transition to $S=1$ will then be very weak owing to the thermal depopulation of the excited crystal-field states. Table II indicates that a similar argument applies when the $|1+\rangle$ excited state is lowest. Up to 77 °K no additional resolved lines, corresponding to transitions between other crystal-field components, are observed on the high-energy side of the 7367.5- and 7301.5-Å lines. The lack of a significant asymmetry of the 7367.5-Å line at 77 °K is consistent with $|\lambda| < 4$ cm^{-1}.

Mollenauer and Schawlow reported emission and absorption lines at 7145 and 7175 Å which were identified by them with transitions involving the higher-energy excited states of the first-neighbor pair.[21] We find the 7175-Å line appears in both polarizations and does not have the appropriate enhancement for 3430-Å excitation expected of a first-neighbor line. A similar lack of an enhancement effect was observed for the spectral region

near 7145 Å. Thus, these lines are not associated with the first-neighbor spectrum.

In Figs. 8 and 9 the wavelengths identified by an asterisk correspond to transitions from the higher-energy excited states. The emission does not, however, involve the first-neighbor pair. For example, these lines appear in both polarizations, being strongest in σ, and do not exhibit the expected enhancement under 3430-Å excitation. The failure to observe the emission from the excited states of the first neighbors is believed to result from (a) the weak intensity relative to the emission from the lowest-energy excited state due to the smaller dipole moments and the Boltzmann factor and (b) the reduction in the enhancement effect due to an increase in energy transfer between pairs and single ions at the higher temperature. These are technical difficulties which can be overcome by using a more intense light source of higher monochromaticity than the monochrometer arrangement used here. For example, a dye laser, N_2 laser, or a Raman-shifted N_2 laser should increase significantly the degree of selective excitation of the first-neighbor system and the higher intensity would allow the use of more dilute samples in which energy transfer is reduced.

A further attempt was made to identify additional first-neighbor lines from the infrared excitation spectrum of the pair luminescence. The monochromatic excitation was isolated using the Czerny-Turner spectrometer, and the luminescence was monitored through a $\frac{1}{4}$-m Bausch and Lomb spectrometer which passed a 90-Å band.

The relative intensities of the lines in the excitation spectra in Fig. 11 show a considerable dependence on the wavelength of the emission. For example, the R lines appeared most strongly in the 7300-Å spectrum, indicating that mainly the R-line vibronics were monitored. The band at 6675 Å which is σ polarized and the unpolarized band at 6587 Å show a similar dependence as the R lines and are associated with the well-known $^2T_1$ single-ion spectrum.[28,29]

First-neighbor emission corresponding to the excitation of the 7145- and 7175-Å lines is not observed. This confirms the earlier conclusions that these lines do not belong to the $S=0$ ground state of the first neighbors. In comparing the 7540- and 7450-Å spectra, the 7540-Å emission is found to be enhanced by a factor 2.5 ± 0.15 for the lines at 6865, 6852, and 6817 Å and the band at 6510 Å. In contrast, the intensity ratio of the R lines is 0.6 ± 0.05. The former is the largest enhancement effect observed, and suggests that these transitions are associated with the first-neighbor pair. Except for the 6852-Å line the transitions are all σ polarized. In higher-resolution absorption measurements, the 6852-Å line is found to consist of two components: an unpolarized line at 6853 Å, and a σ-polarized line at 6852 Å.

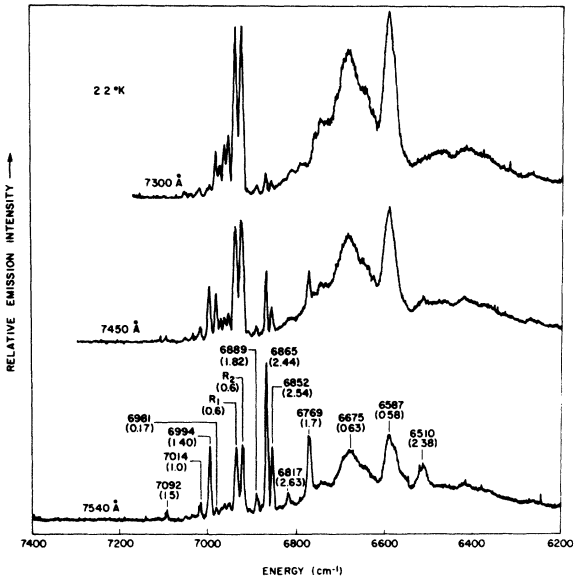

FIG. 11. Infrared excitation spectrum obtained by monitoring the emission at 7300, 7450, and 7540 Å. Several of the wavelengths are shown in the 7540-Å spectrum, and the ratios of 7540- to 7450-Å intensities are shown for the lines. The large enhancement of the 6865-, 6852-, 6817-, and 6510-Å emission suggests that these lines are associated with the first-neighbor pair.

The theory of Sec. IV predicts only a single σ- and π-polarized transitions from the $S=0$ ground state. Thus, while the 6510-Å band may be identified with a transition to the $^2T_1$ level of the first-neighbor pair, it is rather difficult to attribute the remaining lines with transitions to the first-neighbor single excited ^2E levels. Previously, several of these transitions have been identified with the second neighbor. However, the intensity ratios of the second-neighbor lines at 7092 and 6994 Å are only ~1.4. It has already been observed that the first-neighbor lines are wholly polarized, while the second-neighbor lines tend to appear in both polarizations. Thus both the excitation spectra and the polarization data suggest that these lines are first-neighbor lines, which is in disagreement with theory.

Four additional absorption lines from the $S=1$ level are predicted at high temperatures. Experimentally, at temperatures above 77 °K, energy transfer reduces the enhancement effect in the excitation spectrum, and the relative strengh of the R lines is increased. While some temperature-dependent structure is observed near the 6510-Å $^2T_1$ line, no additional lines were observed in the excitation spectrum which could be definitely attributed to the $S=1$ levels of the singly excited ^2E state.

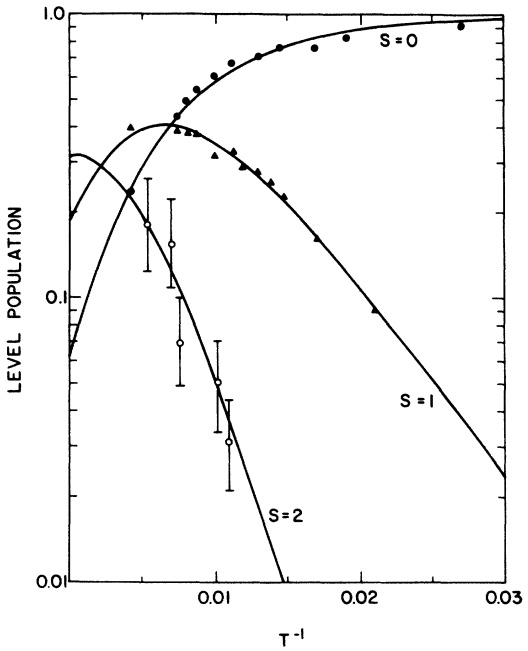

FIG. 12. Curves are the populations of the $S=0$, 1, and 2 levels of the first-neighbor pairs plotted as a function of T^{-1}. The open circles with the error bars are the 7302-Å absorption data of Mollenauer and Schawlow (Ref. 21). The solid circles and triangles are the integrated absorption coefficients, plotted on an arbitrary scale of the 28 694- and 28 980-cm^{-1} transitions to the doubly excited state.

C. Comparison with theory

The two transitions of the first-neighbor pair are quite insufficient to determine the exchange parameters. However, we also have the energy of the excited state from the measured temperature dependence of the 7301.5-Å line.[21] This absorption is now identified as originating on the $S=2-$ ground-state level. Because of the temperature dependence of the population of the other levels, the measured exponential activation energy is a lower limit of the $(S=2-)$-level energy. In order to obtain an estimate of the ground-state exchange, we have used the 123-cm^{-1} separation between the $S=3+$ and $2-$ levels and calculated the absorption as a function of the $S=2-$ energy. The reasonably good fit shown in Fig. 12 is obtained for the parameters $J=54$ cm^{-1} and $j=-8.7$ cm^{-1}. The major uncertainty in determining the exchange energy in this manner is due to the limited accuracy of the absorption measurement. The absorption data of the doubly excited states discussed in Sec. V are also shown by the solid circles in Fig. 12. The exchange splittings are shown in Fig. 4.

Compared with the third and fourth neighbors the value of j relative to J is quite large. However, this value does not appear to be anomalous when compared with the second-neighbor exchange parameters $J=83.6$ cm^{-1} and $j=-9.7$ cm^{-1}.[1,2] The biquadratic exchange term is related to the dependence of the exchange on the vibronic interaction. The unusually large shifts of the first- and second-neighbor lines under stress indicate that the exchange is a strong function of interion separation. The vibronic interaction thus is also expected to be quite strong, leading to a large biquadratic term.

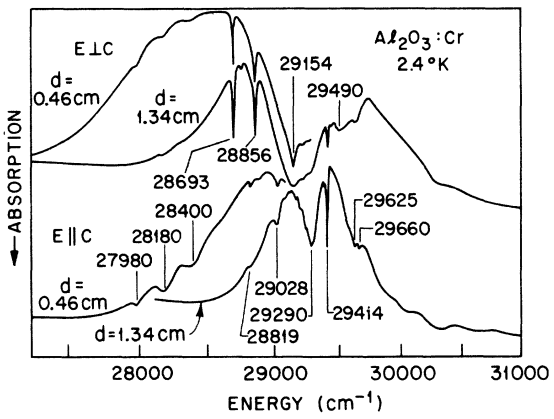

FIG. 13. σ- and π-polarized absorption spectra near twice the R-line energy at 2.4 °K. In order to show detail the absorption from crystals 0.46 and 1.34 cm thick is shown.

V. DOUBLY EXCITED PAIR STATES

A. Absorption spectrum

The polarized absorption spectrum at 2.4 and 77 °K near twice the R-line energy is shown in Figs. 13 and 14. The over-all shape of the transmission curve derives from the combined effects

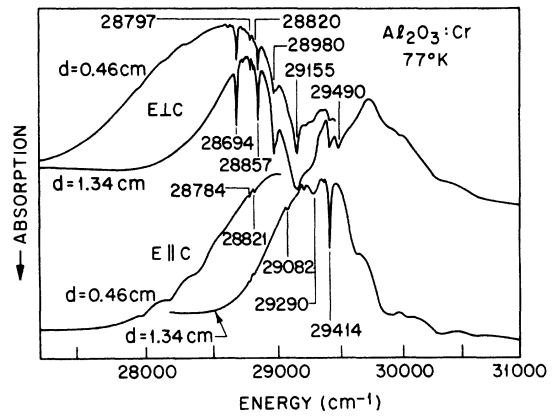

FIG. 14. Polarized absorption spectrum near twice the R-line energy at 77 °K.

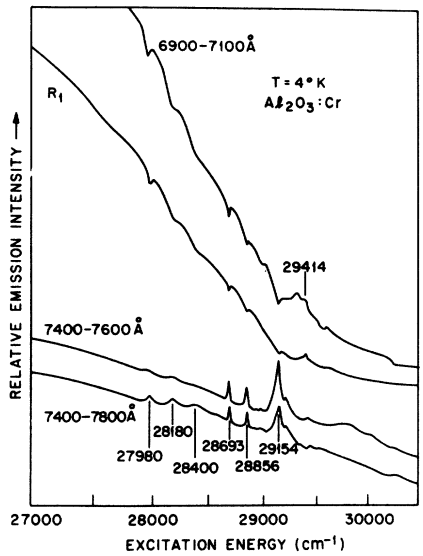

FIG. 15. Excitation spectra at 4 °K of the ultraviolet absorption which was obtained by monitoring the infrared emission in a number of different spectral regions.

of the absorption at low energies due to the tail of the $^4T_1$ band, and at high energies as a result of the combination of crystal absorption and a rapidly decreasing spectral intensity of the lamp. The energies (in cm^{-1}) of several of the stronger transitions are shown, and are in reasonable agreement with the earlier work of Linz and Newnham.[5] The resolution of their spectra was somewhat lower, however, and the line-shape detail is not as evident as in Figs. 13 and 14.

The major features of the σ-polarized spectrum

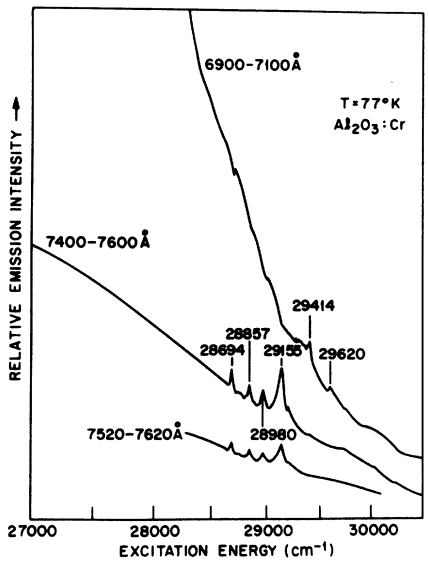

FIG. 16. Excitation spectra of the ultraviolet absorption at 77 °K.

TABLE II. Squares of the matrix elements of the dipole moment to the $|1+\rangle$ singly-excited-states ion in units of $P_\pi^2/12$, $P_\sigma^2/12$, and $x = 10P_{ex}^{X2}/3P_\sigma^2$.

Upper state T	m	ΔE	Lower state $S=0$ π P^2	$S=1$ σ_+ m	σ_+ P^2	σ_- m	σ_- P^2	$S=2$ π m	π P^2
1	1	$\lambda/4$		1	$5+x$	0	5	2	6
−1	−1	$\lambda/4$		0	5	−1	$5+x$	−2	6
−1	0	0		1	5	0	x	−1	3
1	0	0		0	x	−1	5	1	3
−1	1	$-\lambda/4$	4			1	$5+x$	0	1
1	−1	$-\lambda/4$	4	−1	$5+x$			0	1

at 2.4 °K are the two sharp first-neighbor lines at 28 693 and 28 856 cm^{-1} and the strong band at 29 154 cm^{-1} which originate on the $S=0$ level. The intensity of these lines has decreased at 77 °K and a new line has appeared at 28 980 cm^{-1} which originates on the $S=1$ level of the first-neighbor pair. Several additional weak lines appear between 28 790 and 28 850 cm^{-1}.

The line at 29 414 cm^{-1} appears most strongly in π polarization, and has previously been identified with a single-ion transition to the $^2A_1$ state.[7-9] Vibronic and pair transitions of this line are observed above 29 600 cm^{-1}.

In π polarization there is a group of three broad lines at 27 980, 28 180, and 28 400 cm^{-1}. There is also a relatively weak line at 28 819 cm^{-1} with predominantly π-polarized vibronics at 29 028 and 29 290 cm^{-1}. These lines become weaker as the temperature is raised and several weak additional lines appear in both the σ and π spectra. The energies of these lines are quite close to twice the R-line energy (~28 835 cm^{-1}) and this absorption is identified with doubly excited pair transitions of neighbors more distant than the first.

B. Excitation spectrum

Information about the centers responsible for the absorption was obtained from the excitation spectrum of the pair luminescence. Polarized monochromatic uv radiation from the 1-m Czerny-

TABLE III. Squares of the matrix elements of the dipole moment to the $|1-\rangle$ singly excited state in units of $P_\pi^2/12$ and $P_\sigma^2/12$.

Upper state T	m	ΔE	Lower state $S=0$ σ_+ P^2	σ_- P^2	$S=1$ π m	P^2	$S=2$ σ_+ m	P^2	σ_- m	P^2
1	1	$\lambda/4$		4			1	3	0	1
−1	−1	$\lambda/4$	4				0	1	−1	3
−1	0			4	−1	5	1	3	0	4
1	0		4		1	5	0	4	−1	3
−1	1	$-\lambda/4$			0	5	2	6	1	3
1	−1	$-\lambda/4$			0	5	−1	3	−2	6

TABLE IV. Squares of the matrix elements of the dipole moment to the $|2+\rangle$ singly excited state in units of $P_\pi^2/12$ and $P_\sigma^2/60$.

Upper state T	Upper state m	Lower state ΔE	$S=1$ σ_+ m	$S=1$ σ_+ P^2	$S=1$ σ_- m	$S=1$ σ_- P^2	$S=2$ π m	$S=2$ π P^2	$S=3$ σ_+ m	$S=3$ σ_+ P^2	$S=3$ σ_- m	$S=3$ σ_- P^2
1	2	$\lambda/2$			1	6			2	20	1	4
−1	−2	$\lambda/2$	−1	6					−1	4	−2	20
1	1	$\lambda/4$	1	3	0	3	2	2	1	32	0	12
−1	−1	$\lambda/4$	0	3	−1	3	−2	2	0	12	−1	32
−1	0	0	1	1	0	4	−1	3	1	24	0	12
1	0	0	0	4	−1	1	1	3	0	12	−1	24
−1	1	$-\lambda/4$			1	3	0	3	2	20	1	32
1	−1	$-\lambda/4$	−1	3			0	3	−1	32	−2	20
−1	2	$-\lambda/2$					1	2	3	60	2	20
1	−2	$-\lambda/2$					−1	2	−2	20	−3	60

Turner spectrometer was incident on the crystal, and the infrared luminescence was detected at right angles. The luminescence was isolated using Corning glass and several interference filters in front of the photomultiplier tube. The emission lines of interest are the R line at 6934 Å, the 7009-Å fourth-neighbor line, the 7041-Å third-neighbor line, the 7450-Å second-neighbor line, and the 7540-Å first-neighbor line.

Several excitation spectra are shown in Figs. 15 and 16. In Fig. 15 the 6934-Å emission increases rapidly at low energies owing to excitation into the $^4T_1$ band. The one sharp feature is the line at 29 414 cm^{-1} corresponding to the single-ion doublet absorption. The strong lines in the absorption spectrum appear as self-absorption dips in the $^4T_1$-band tail. The excitation spectrum of the 7009- plus 7041-Å emission shows additional structure near 29 414 cm^{-1}. These lines are absent in the 7009-Å spectrum and are thus identified with the single excited pair states of the third neighbor.

The lines of interest appear when the 7540- plus 7450-Å emission is monitored. Tilting the interference filter shifts its transmission band to shorter wavelengths, and the intensity of the sharp lines are greatly reduced when the filter no longer transmits the 7540-Å line. The excitation spectrum also is observed with a filter transmitting from 7520 to 7620 Å. Consequently, the strong lines are identified with transitions from the $S=0$ level of the first-neighbor pair. The doubly excited pair states of the second neighbor have not been clearly observed in the excitation spectrums of the 7450-Å emission.

At 77 °K the 28 980-cm^{-1} line also appears solely in the spectrum of the 7540-Å emission, confirming its identity as a first-neighbor transition which originates on the $S=1$ level. The lower trace of Fig. 15 was obtained using Corning 7-69 and 2-64 filters which transmit for $\lambda > 7400$ Å and contain the three lower energy peaks. Analysis with several interference filters indicates the emission is mainly in a broad band centered at ~7590 Å.

The sloping background of the excitation curves also deserves some comment. The slope is in part determined by the spectral dependence of the lamp and the opening of the spectrometer slits which govern the excitation into the $^4T_1$ single-ion band. The slope then appears in the pair spectrum because of $^4T_1$ absorption of the pair as well as from energy transfer from the single ions to the pairs. Figure 15 shows that the effect of the $^4T_1$ band is quite large for the third- and fourth-neighbor pairs, indicating the transfer from the single ion is considerably greater than to the first two neighbors. Comparison of the slopes of the curves in Figs. 15 and 16 shows that the transfer increases with temperature.

C. Effects of uniaxial stress and temperature

The dependence on uniaxial stress applied along the c axis was measured at 77 °K. Stresses up to

TABLE V. Squares of the matrix elements of the dipole moments to the $|2-\rangle$ singly excited state in units of $P_\pi^2/60$, $P_\sigma^2/12$, and $y = 6P_{ox}^{X2}/P_\sigma^2$.

Upper state T	Upper state m	Lower state ΔE	$S=1$ π m	$S=1$ π P^2	$S=2$ σ_+ m	$S=2$ σ_+ P^2	$S=2$ σ_- m	$S=2$ σ_- P^2	$S=3$ π m	$S=3$ π P^2
1	2	$\lambda/2$			2	$4+y$	1	2	3	60
−1	−2	$\lambda/2$			−1	2	−2	$4+y$	−3	60
1	1	$\lambda/4$			1	$1+y$	0	3	2	40
−1	−1	$\lambda/4$			0	3	−1	$1+y$	−2	40
−1	0	0	−1	1	1	3	0	y	−1	24
1	0	0	1	1	0	y	−1	3	1	24
−1	1	$-\lambda/4$	0	3	2	2	1	$1+y$	0	12
1	−1	$-\lambda/4$	0	3	−1	$1+y$	−2	2	0	12
−1	2	$-\lambda/2$	1	6			2	$4+y$	1	4
1	−2	$-\lambda/2$	−1	6	−2	$4+y$			−1	4

TABLE VI. Squares of the exchange-induced electric dipole matrix elements to the $|0(-)\rangle$ doubly excited states in units of $P_{ex}^{X'2}/36$.

Upper state Ψ	Lower state m	ΔE	$S=0$ σ_+ m	P^2	σ_- m	P^2
$\lvert e_-e_-\rangle$	0	0	0	9		
$\lvert e_+e_+\rangle$	0	0			0	9

130 kg/mm^2 were routinely applied. For a stress of 100 kg/mm^2 the shifts of the $S=0$ lines at 28 694, 28 857, and 29 155 cm^{-1} are -6.5 ± 0.2, -5.2 ± 0.2, and -9 ± 0.1 cm^{-1}, respectively, and the shift of the $S=1$ line at 28 980 cm^{-1} is -8.3 ± 0.2 cm^{-1}. The shifts are not the same, suggesting that the absorption involves different electronic levels.

The observed shift contains contributions from the change in the ground- and excited-state exchange, as well as the change in the crystal-field splitting. As a first-order approximation we can use two times the single-ion shift as a measure of the crystal-field contribution to the shift of the doubly excited states. The single-ion R_1- and R_2-line shifts, according to Feher and Sturge, are -1.75 and -2.35 cm^{-1} per 100 kg/mm^2, respectively.[30] The observed shifts of the doubly excited states are about twice as large as the values calculated using the single-ion crystal-field shifts. Thus, in contrast to the singly excited pair states which showed very large shifts, the stress dependence of the exchange in the ground and excited states of the doubly excited pair approximately cancels.

The integrated absorption coefficients of the 28 694-, 28 857-, and 28 980-cm^{-1} lines were measured as a function of temperature using a thin sample of 0.9 wt% Cr^{3+}. The 28 694- and 28 980-cm^{-1} data which are shown by the solid circles in Fig. 12 were multiplied by constants in order to bring them into coincidence with the level-population curves. The temperature dependence of the 28 857-cm^{-1} follows the $S=0$ curve when the effect of several weaker satellite lines is subtracted, and the strong 29 155-cm^{-1} absorption, which was not measured as accurately, has a qualitatively similar dependence. The absorption data appear to agree reasonably well with the temperature dependence of the population. Comparing the absorption curves with the $S=0$ and 1 populations of the second neighbors, with which Engstrom had identified this absorption,[22] gave especially for the $S=1$ data considerably poorer agreement. We should point out, however, that while it is relatively easy to obtain excellent agreement between the population curves and the absorption data when the level energies are known, it is considerably more difficult to obtain the energies very accurately from the absorption data as we have done here.

D. Comparison with theory

In the bilinear-exchange approximation, the $S=0$ and 1 doubly excited states consist of three exchange-split levels, and the splittings of the $S=1$ levels are $-\frac{1}{3}$ the splittings of the $S=0$ levels. Each level is doubly degenerate and, in addition, the $S=1$ levels have the usual threefold spin degeneracy. The spin-dependent dipole moment couples only to the $|0(-)\rangle$ and $|1(+)\rangle$ states with σ polarization. Experimentally we have identified the three σ transitions at 28 694, 28 857, and 29 155 cm^{-1} with the $S=0$ level, and the 28 980-cm^{-1} σ transition with the $S=1$ level. We tentatively identify the latter two transitions with the allowed spin-dependent dipole absorption. The relative strengths of the two absorption lines agree with this assignment. At 70 °K the ratio of the $S=1$ to $S=0$ integrated absorption coefficients is 0.17 ± 0.05, and this compares very well with the ratio of 0.175 obtained from the theoretical dipole moments and the level populations shown in Fig. 12. According to the theory the separation between the two lines gives the difference in the $S=0$-to-$S=1$ exchange splitting due to J in the ground and doubly excited states. The observed separation is 175 cm^{-1} and using the observed 111-cm^{-1} $S=0$-to-$S=1$ ground-state splitting, this results in the $|1(+)\rangle$ state lying 64 cm^{-1} below the $|0(-)\rangle$ state. The observed sign of the splitting is thus opposite to the sign predicted from bilinear exchange (Fig. 3). This reversal is not simply explained by spin-orbit–crystal-field interactions or by biquadratic exchange.

A further indication that there is a serious problem with the interpretation of the doubly excited states is the observation that the energies of the $S=0$ lines at 28 694 and 28 857 cm^{-1} are well below the strong line at 29 155 cm^{-1}. If the former two

TABLE VII. Squares of the exchange induced electric dipole matrix elements to the $|1(+)\rangle$ doubly excited states in units of $P_{ex}^{X'2}/36$.

Upper state Ψ	Lower state m	ΔE	$S=1$ σ_+ m	P^2	σ_- m	P^2
$\lvert e_-e_-\rangle$	1	$-\lambda$	1	5		
	0	0	0	5		
	-1	λ	-1	5		
$\lvert e_+e_+\rangle$	1	λ			1	5
	0	0			0	5
	-1	$-\lambda$			-1	5

transitions are assumed to involve the $|0+\rangle$ and $|0-\rangle$ excited states, respectively, the identification is quite inconsistent with the theory of Sec. III. Furthermore, the theory also does not explain the weak dipole moments of these transitions. The transitions to the $|S\pm\rangle$ states are forbidden because of a cancellation of the single-electron–single-electron contributions of the spin-dependent dipole moment. For example, the transitions to the $|1+\rangle$ and $|0-\rangle$ states vanish because the three nonzero dipole moments, one of which is given by Eq. (17), are directed from the center of the oxygen triangle towards the three oxygen ions, and the sum of the three dipole vectors vanishes. The transitions would have a nonvanishing spin-dependent dipole moment if the trigonal rotational symmetry were removed. This could, for example, result from a distortion along the X axis. The transitions to the $|0+\rangle$ and $|1-\rangle$ states, on the other hand, are forbidden by the interchange symmetry of the ions. Removal of this symmetry, by movement of one of the ions along the trigonal axis, would also make this transition allowed. Such distortions may arise from the Jahn–Teller effect.[31] The case of an interaction between two octahedrally coordinated E_g-state ions and a vibrational mode has been discussed by Novak.[32] The Jahn–Teller effect for a pair of T_{1g} and T_{2g} ions has been discussed by Novak and Stevens,[33] and has been applied to the two-exciton spectrum of $KMnF_3$ by Fujiwara.[34] These calculations, unfortunately, consider only the lattice-crystal-field contribution to the energy shift. For a pair of magnetic ions, a small change in the equilibrium position may produce a significant modification of the exchange, which in turn contributes a larger shift to the energy levels than the corresponding change due to the crystal field.

VI. SUMMARY AND CONCLUSIONS

In this paper we have compared the theory of bilinear exchange of the first-neighbor pair of ruby with previous as well as new experimental data. Because the symmetry of the pair is high, the number of independent bilinear-exchange terms is reduced to two, and the energies of the excited states depend on the exchange parameters as shown in Figs. 2 and 3. While the symmetry helps to simplify the theory, it increases the experimental problems. For example, the number of transitions which are allowed by the exchange-induced dipole mechanism are reduced. In addition, the magnitude of this dipole moment to the singly-excited states is reduced by a fortuitous near cancellation of the single-electron dipole moments. Consequently, the dipole strength of these transitions derives mainly from the single-ion mechanism. The absence of the intensity enhancement due to the exchange effect makes it considerably more difficult to detect the first-neighbor transitions in the vibronic background of the single ions and the other pairs. Exchange-striction effects are quite large in the ground state, and are probably also significant in the excited states. This is illustrated by the large shifts of the lines under uniaxial compression along the crystal axis. Exchange striction adds additional parameters to the theory, and shifts the energy levels from the bilinear-exchange values. The corresponding dependence of the equilibrium position of the ions on the value of the spin affects the degree of vibronic coupling. This affects the intensities of the zero-phonon lines and complicates the comparison of the relative intensities.

A significant increase in the pair luminescence, relative to single-ion excitation is observed when the doubly excited states are excited. By comparing the intensities of the emission for excitation into these levels, we have been able to confirm the σ-polarized line at 7301.5 Å as an electronic first-neighbor transition between the $|2-\rangle$ states. The π-polarized transition at 7540 Å is attributed to a vibronic of the weak π-polarized electronic $|2-\rangle$-to-$|3+\rangle$ transition at 7367.5 Å. The remaining three transitions which were previously identified with the first-neighbor spectrum do not show an enhancement effect and thus are not associated with the first-neighbor pair.

Using the energy difference between the $|3+\rangle$ and $|2-\rangle$ states as well as the temperature dependence of the absorption of the 7301.5-Å line, the ground-state exchange parameters are found to be $J=54$ and $j=-8.7$ cm^{-1}, and the ground-state energies are shown in Fig. 4. The 7301.5-Å absorption is quite weak and the measured temperature dependence is relatively inaccurate; consequently, the precision to which the exchange parameters are determined is probably quite low. The more accurately determined temperature dependences of the $S=0$ and 1 doubly excited states are, however, in quite good agreement with this assignment.

Thus some progress has been made in understanding the first-neighbor spectrum, and a new ground-state assignment has been found. However, both the theory of the excited state as well as the experimental determination of these levels is not yet complete. The theory needs primarily to be extended to include the excited-state analog of the ground-state exchange-striction effects. This was not done in this paper because of the limited number of excited-state levels which were observed. The weak transitions to the higher-energy singly-excited-state transitions can probably be best observed in the excitation spectrum of the 7540-Å emission, or in one of the other vibronic

bands of the 7367.5-Å line. By using a tunable laser source, as well as considerably more dilute Cr^{3+} concentrations, the large selective enhancement effect should be observable up to temperatures where the excited levels of the ground state are populated. This should allow for the identification of the $S=2$ as well as the $S=1$ singly excited levels. There is also the possibility of observing the other transitions by reducing the cancellation of the symmetry-forbidden exchange-induced dipole moments by applying an external stress to the crystal. Finally, the magnetic contributions to a possible Jahn–Teller effect in the doubly excited state cannot be ruled out.

ACKNOWLEDGMENTS

The author is grateful to M. H. L. Pryce for a copy of his unpublished paper on exchange interactions which initially stimulated this work. The author is indebted to M. Naito for a report prior to publication of his theory of the pair spectrum in ruby, to L. F. Mollenauer and M. D. Sturge for a number of helpful discussions, and to D. L. Wood and J. C. Koo for the loan of several crystals. The technical assistance of L. Kopf is gratefully acknowledged.

APPENDIX: TRANSITION MOMENTS

Tables II–VII give the squares of the dipole moments of the single-ion and exchange-induced dipole-moment mechanism to the single and doubly excited pair states. The lower-energy states are denoted by S and m. The upper states are denoted by S, m, the $(\pm)$ parity under interchange of the ions, the orbital component of $e_M(T=\pm 1)$, and the fine-structure energy from Eq. (6). The transition moments to the single excited states have previously been given in this form by Pryce,[3] and in a generalized form by Naito.[4]

[1]For a recent review see R. C. Powell and B. Di Bartolo, Phys. Status Solidi A 10, 315 (1972).
[2]P. Kisliuk, N. C. Chang, P. L. Scott, and M. H. L. Pryce, Phys. Rev. 184, 367 (1969).
[3]M. H. L. Pryce (unpublished). The theory of Pryce has recently been applied to Cr^{3+} pairs in $ZnGa_2O_4$ [G. G. P. van Gorkom, J. C. M. Henning, and R. P. van Stapele, Phys. Rev. B 8, 955 (1973); G. G. P. van Gorkom, Phys. Rev. B 8, 1827 (1973)].
[4]M. Naito, J. Phys. Soc. Jap. 34, 1491 (1973).
[5]A. Linz and R. E. Newnham, Phys. Rev. 123, 500 (1961).
[6]S. Sugano and Y. Tanabe, J. Phys. Soc. Jap. 13, 880 (1958).
[7]C. S. Naiman and A. Linz, in *Proceedings of the Symposium on Optical Masers* (Polytechnic Institute of Brooklyn, Brooklyn, N.Y. 1963), p. 369.
[8]F. Gires and G. Mayer, J. Phys. Radium 7, 492 (1961).
[9]T. M. Dunn and A. H. Francis, Phys. Rev. Lett. 25, 705 (1970).
[10]R. W. G. Wyckoff, *Crystal Structures*, 2nd ed. (Wiley, New York, 1964), Vol. 2.
[11]See, for example, P. W. Anderson, *Solid State Physics*, edited by F. Seitz and D. Turnbull (Academic, New York, 1963), Vol. 14, p. 99.
[12]D. S. McClure, J. Chem. Phys. 36, 2757 (1962).
[13]D. S. McClure, J. Chem. Phys. 38, 2289 (1963).
[14]For a discussion of exchange see, for example, J. Owen and E. A. Harris, *Electron Paramagnetic Resonance*, edited by S. Geschwind (Plenum, New York, 1972), Chap. 6.
[15]E. A. Harris and J. Owen, Phys. Rev. Lett. 11, 9 (1963).
[16]E. A. Harris, J. Phys. C 5, 338 (1972).
[17]M. E. Lines, Solid State Commun. 11, 1615 (1972).
[18]Y. Tanabe, T. Moriya, and S. Sugano, Phys. Rev. Lett. 15, 1023 (1965); K. I. Gondaira and Y. Tanabe, J. Phys. Soc. Jap. 21, 1527 (1966); Y. Tanabe and K. I. Gondaira, J. Phys. Soc. Jap. 22, 573 (1967); N. Fuchikami and H. Ono, J. Phys. Soc. Jap. 34, 360 (1973). See also R. Loudon, Advan. Phys. 17, 243 (1968).
[19]J. P. van der Ziel, Phys. Rev. Lett. 26, 766 (1971).
[20]J. P. van der Ziel, Phys. Rev. B 4, 288 (1971).
[21]L. F. Mollenauer and A. L. Schawlow, Phys. Rev. 168, 309 (1968).
[22]H. Engstrom, thesis (University of California, Berkeley, 1972) (unpublished).
[23]H. Engstrom and L. F. Mollenauer, Phys. Rev. B 7, 1616 (1973).
[24]J. P. van der Ziel, J. Chem. Phys. 57, 2442 (1972).
[25]T. Kushida and Y. Tanaka, Solid State Commun. 11, 1341 (1972).
[26]Some of these shifts are evident in Fig. 7 of A. A. Kaplyanskii and A. K. Przhevuskii, Fiz. Tverd. Tela 9, 257 (1967) [Sov. Phys.-Solid State 9, 190 (1967)].
[27]D. F. Nelson and M. D. Sturge, Phys. Rev. 137, 1117 (1965).
[28]J. Margerie, Compt. Rend. 255, 1598 (1962).
[29]R. M. McFarlane, J. Chem. Phys. 39, 3118 (1963).
[30]E. Feher and M. D. Sturge, Phys. Rev. 172, 244 (1968).
[31]M. D. Sturge, Solid State Phys. 20, 92 (1967).
[32]P. Novak, J. Phys. Chem. Solids 30, 2357 (1969).
[33]P. Novak and K. W. H. Stevens, J. Phys. C 3, 1703 (1970).
[34]T. Fujiwara, J. Phys. Soc. Jap. 34, 36 (1973); 34, 1180 (1973).